Dynamics at the nanoscale

A.M. Stoneham, J.L. Gavartin *

London Centre for Nanotechnology, Department of Physics and Astronomy, University College London, Gower Street, London WC1E 6BT, United Kingdom

Abstract

However fascinating structures may be at the nanoscale, time-dependent behaviour at the nanoscale has far greater importance. Some of the dynamics is random, with fluctuations controlling rate processes and making thermal ratchets possible. Some of the dynamics causes the transfer of energy, of signals, or of charge. Such transfers are especially efficiently controlled in biological systems. Other dynamical processes occur when we wish to control the nanoscale, e.g., to avoid local failures of gate dielectrics, or to manipulate structures by electronic excitation, to use spin manipulation in quantum information processing. Our prime purpose is to make clear the enormous range and variety of time-dependent nanoscale phenomena.
© 2006 Elsevier B.V. All rights reserved.

1. Introduction

The nanoscale is extraordinarily dynamic. Even a cluster of 100 atoms in thermal equilibrium at room temperature will have root mean square volume fluctuations of the order of 1%, similar to the root mean square volume fluctuation of a human breathing normally, although the timescales differ by a factor of order 10^{12}. Nanoparticles grow, restructure, and interact. Excitation leads to electronic processes on the femtosecond timescale, relaxation processes on the picosecond timescale, and optical and non-radiative transitions on the nano- and microsecond timescales. Biological processes can involve energy propagation, signal propagation and the controlled and correlated movements of atoms. Molecular motors appear to operate with relatively soft components. Solitons appear to move modest amounts of energy with minimal loss, even in living humans. Enzyme actions can involve proton tunnelling. The initial processes when large molecule meets a receptor are determined primarily by shape and size, but depend strongly on fluctuations. For small molecules, other factors are involved: for

serotonin, the process may be proton transfer; for scent molecules at olfactory receptors, inelastic electron tunnelling may be the critical phenomenon. Quantum computing based on condensed matter systems is inherently nanoscale, since entanglement is effective only on the submicron level. It is also inherently dynamic, in that manipulations of qubits have to be faster than decoherence (quantum dissipation) mechanisms. Indeed, quantum information processing and life processes have common ground in exploiting behaviour far from equilibrium.

In both physical and biological nanoscale systems, time-dependent processes take on a special importance. Some time dependence is unavoidable. The functionality of these systems depends both on the nanoscale object itself, and on its working environment, so there are consistencies that have to be achieved. It can be useful to distinguish between natural and operational timescales (cf. the length scales discussed by Stoneham and Harding [1]. *Natural time scales* might be the time it takes for sound to cross a nanodot, or spontaneous optical emission at the sum rule limit. *Operational time scales* are designed and made, often with difficulty. In a state-of-the-art microelectronics device, the structures have sizes determined partly by nature, partly by compatibility with previous generations of device, and partly by the laws of physics and the art of the possible. The materials and their organisation are designed to maximise signal speeds, delay memory decay, and

---

* Corresponding author.
  E-mail addresses: a.stoneham@ucl.ac.uk (A.M. Stoneham),
j.gavartin@ucl.ac.uk (J.L. Gavartin).

keep energy dissipation under control. *Biological* systems evolve to make operational timescales seem natural. But how is this done, and can we benefit from understanding?

We shall discuss some of the many time-dependent processes associated with nanoscale objects. These include two systems at the smaller end of the nanoscale. The II–VI quantum dots of perhaps 200 ions show a wealth of time-dependent processes, but mainly ones for which a classical description is useful. The other example is usually described classically, yet for which quantum behaviour appears crucial: how do scent molecules (rarely, if ever, bigger than 100 atoms) provoke receptors, and initiate signals that ultimately reach the brain?

2. Time-dependent behaviour and the II–VI nanodot

2.1. Growth and what stops it

Microbial synthesis offers a striking method for large-scale production of CdS nanodots [2]. But why do the dots stop growing and stay nanosized, with sizes as uniform as can be achieved by sophisticated chemical methods? If ice and mushrooms can break up concrete, how can soft biomaterials constrain size when there seems to be a large thermodynamic force to grow? This is an important issue in biology, where the shapes of structures (like shells) determine their function. Sometimes there is *clever control*, when organisms exploit the capabilities of DNA. Protein cages are crucial in the synthesis of magnetic nanoparticles like the single domain ferrimagnetic Fe_3O_4 found in magnetotactic bacteria [3]. The mammalian ferritins are built from two types of subunit (H, L) that align in antiparallel pairs to form a shell with narrow (~ 3 Å) channels. One class of channel is hydrophobic, the other hydrophylic. Mineralisation involves iron oxidation, hydrolysis, nucleation, and growth. The Fe ions enter the cage via the hydrophilic channels, and it is presumably electrostatics that controls entry and so limits growth. The outer entrance is a region of positive potential, guiding cations into the cage until the ferritin fills the internal cavity rather precisely. It is possible that similar mechanisms operate in other systems where shape matters, possibly CdS. Size alone can be controlled in other ways, e.g., through surface nucleation barriers (Frank 1952), limits to materials supply, or blocking of growth sites by a capping species. Access to a nanodot surface is important in medical applications, and we remark that chaperonin proteins form ATP-responsive barrel-like cages for nanoparticles [4].

2.2. Vibrational spectra of quantum dots

For the smallest ionic dots, as observed in molecular beams, there is evidence that crystal structure can differ from the bulk form. Partly this is associated with large electric fields in such dots. Are the vibrational features of nanoclusters also qualitatively different from the bulk? Can one identify effects of discrete phonon spectra [5]? Are there modes that exist with frequencies higher than those of the corresponding bulk zone-centre LO phonon [6]? If such effects exist, can we associate them with the bulk or the surface, or is there some intimate mixture?

All nanodots – whether metallic, covalent or ionic – will show effects of confinement. As regards differences between ionic (say 6-fold coordinated rock-salt) and covalent (4-fold coordinated zinc blend) systems, the trends in phonon confinement are parallel to electron confinement in some ways. Thus there is a substantial electron confinement (band gap opening) at the appropriately terminated silicon surface, whereas one finds surface states in the band gaps of MgO or NaCl. The same applies to surface phonons. Ab initio calculations predict a surface band at ~ 4 meV above the maximum bulk frequency at the silicon (2×1) surface [7,8], but the (001) surface vibrations of NaCl and MgO do not exceed the energy of the bulk LO phonons. We may illustrate this by considering the vibrational dynamics of NaCl and ZnS nanoclusters. Fig. 1 shows the vibrational density of states (DOS) of various NaCl nanocrystals calculated using shell model lattice dynamics.

We see that only those cubic nanocrystals with only (001) type surfaces have a vibrational DOS similar to that of the bulk material. In contrast, the faceted clusters, with less stable surfaces, show modes with frequencies up to 5 meV above $\omega_{LO} = 32$ meV. Although specific nature of the modes depends on details of surface termination, all faceted clusters have both surface-like and bulk-like high frequency modes. The bulk-like modes probably result from constructive interference of the surface modes localized near the opposite high index faces of a crystallite. If so, such modes should eventually disappear in larger nanocrystallites.

The vibrational DOS for the zinc-blende like $(ZnS)_{47}$ cluster (Fig. 2) is obtained using Born–Oppenheimer molecular dynamics within plane wave density functional theory [9–11]. Here a vibrational mode is observed at around 56 meV, well above
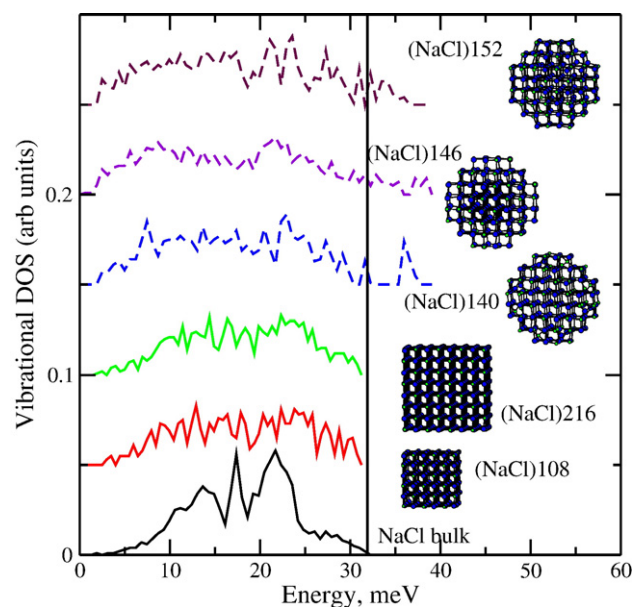

Fig. 1. Shell model vibrational densities of states of selected NaCl nanocrystals. Cubic nanocrystals $(NaCl)_{108}$ and $(NaCl)_{216}$ have no vibrations with frequencies higher than the bulk $\omega_{LO} = 32$ meV, while the faceted clusters $(NaCl)_{140}$, $(NaCl)_{146}$ and $(NaCl)_{152}$ display high frequency tails.
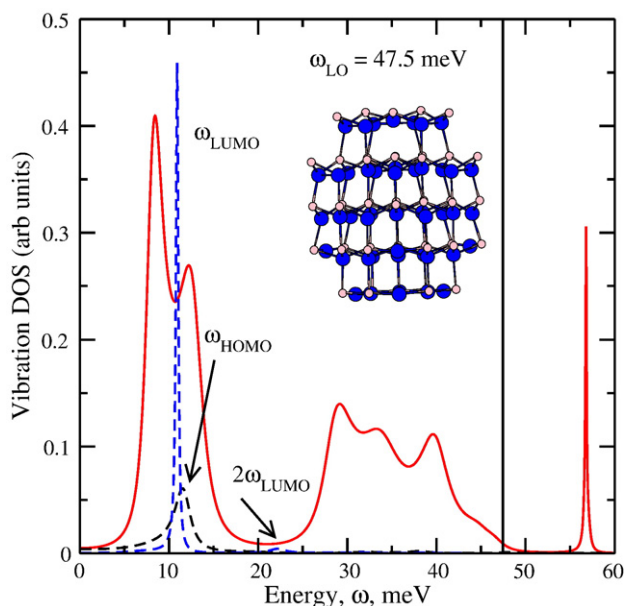
Fig. 2. Vibrational density of states of the $(ZnS)_{47}$ cluster obtained from the ab initio molecular dynamics at $T=300$ K. Also shown are the power spectra of time dependence of HOMO and LUMO energies.

the bulk LO phonon of 47.5 meV [12]. The presence of high frequency modes is in line with earlier shell model predictions [6].

Clearly, modes with $\omega > \omega_{LO}$ (bulk) do exist at least in some nanoclusters. How universal this is for small nanodots needs to be investigated further. An important unresolved question is how strongly these vibrations couple to the electronic excitations. The standard pictures of electron–phonon coupling would suggest that the dominant coupling in ZnS would be with the LO modes around 47 meV. Yet analysis of the dynamics of the electron eigenstates (Fig. 2), shows that both occupied and empty single-particle states couple primarily to a much softer mode at ~ 11 meV. The second harmonic of this mode (coupling to 2 phonons) is also clearly seen at ~ 22 meV. Calculations do show a much weaker coupling of the highest occupied (HOMO) and lowest unoccupied (LUMO) molecular orbitals to other modes, including the LO-like features at around 45 meV (not seen at this scale). No coupling is evident to the high frequency mode at 56 meV, which suggests that this mode might be silent.

2.3. Dynamics and nanocrystal structure

One striking observation [13] is that the electron diffraction peak for an individual dot can appear to switch off for periods of a few seconds or longer. This can happen even for Au dots. Just what causes this effect is still unsettled, but the several possible mechanisms identify possible time-dependent processes.

A first model would simply involve rotation of the dot. This sounds credible in a soft matrix, like a polymer, or on a surface, when rotation is easy but less so in apparently rigid systems such as silica glass. However, soft rotation-like and cage modes below 5 meV were predicted for very small $(ZnS)_{47}$ dots embedded into amorphous SiO_2 matrix [6] (Fig. 3). Our subsequent analysis

showed these vibrations may be coupled to the floppy a-SiO_2 modes believed to be universal in glasses [14,15]. One would expect this frequency to fall rapidly with dot size, since the relevant mode force constant will be roughly proportional to the number of bonds between the dot and adjacent atoms, i.e., to the area, and hence $\sim R^2$ for a dot of radius R, whereas the moment of inertia increases as R^5. The loss of diffraction peak needs the dot to change its vibrationally-averaged orientation to another, and this will be easier when there are low-frequency rotational modes.

Even if there are soft rotational modes, it is hard to understand what forces drive rotation. Heating and thermal expansions in inorganic systems give compressive forces, but do not readily cause rotation. A second model for a dot on a substrate might involve photochemical effects on adsorbed species (e.g., H_2O, or C oxidation), where there could be a well-defined asymmetry to cause the particle to rotate. A third model supposes melting or quasi-melting. "Quasi-melting" sometimes means melting only in an outer surface or interfacial layer, with an unmelted core. If so, the diffraction peak should not be lost, though it might fall in intensity. Asymmetric (local) melting might cause rotation, as in the second model. However, in a liquid, one would expect the diffraction pattern to streak before it vanishes. One also expects the acoustic (thermal) mismatch between dot and host to matter: big differences between densities or elastic constants will keep the dot hot for longer. There should also be some dependence on the geometric match of dot and matrix structures. The switch-off time should depend on excitation rate. Melting (like process 1 and perhaps 2) may happen in metallic dots, as observed, as well as in semiconducting or insulating ones.

A fourth model, not for metals, presumes a change of geometry following charge transfer. The idea [16] is that the electron beam causes charge transfer within the (non-metallic) dot, analogous to some of the charge transfers inferred in spectroscopy. This shift of an electronic charge from one site to another causes ionic polarisation within the dot, affecting the diffraction peak. Essentially, charge transfer transition takes the dot to a second,
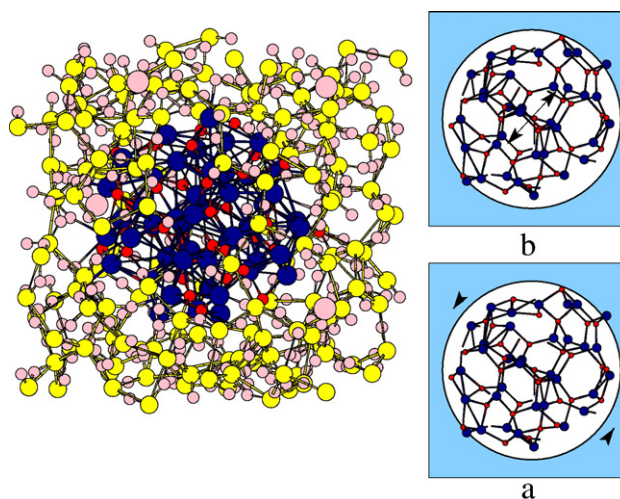

Fig. 3. Atomistic model of the $(ZnS)_{47}$ cluster embedded into a-SiO_2 matrix. Six low-frequency modes — 3 rotational (a) and 3 cage modes (b) of the cluster are identified at frequencies below 5 meV.

metastable, state which could easily survive a reasonable time. Simple molecular dynamic models show this process should work for very small dots of a few tens of ions. Structural changes are seen even under much less energetic optical excitation: the sub-band gap irradiation by 2.33 eV photons causes an orthorhombic to cubic transformation in CdS [17]. If ionisation occurs, a Coulomb explosion has been observed for microclusters in molecular beams. Typically, the "Coulomb explosion" occurs when there are two holes present and less than some critical number of atoms, roughly 20 molecular units for NaI, 30 Pb atoms, or 52 Xe atoms [18].

2.4. Intermittency and luminescence

The spectroscopy of II–VI quantum dots has been the subject of many studies (see, e.g., Zunger (this meeting), [19,20] and lies outside our discussion of dynamics. Experimental spectroscopy gives some striking indications of dynamical processes and their rates, as we now discuss.

Many studies of II–VI dot luminescence (e.g., [21–24]) show intermittency: under continuous laser excitation, there are periods for which any one dot "goes off", ceasing to luminesce. The probability distribution for finding any single dot in a dark or a fluorescing state for time t decays as $\sim t^{-\alpha}$ with $\alpha \sim 1.4$–1.5 in both cases [25]. This inverse power behaviour has been observed in variously capped CdSe [34], CdTe, PbS [26] nanocrystals and nanorods in Si [27] and even in selected carbon nanotubes [28]. Over wide ranges of situations, α varies little on laser power, temperature or particle radius [29]. While there is still debate on the universality range of the inverse power decay, with both short- and long-time cutoffs reported [30]), the statistical patterns of quantum dot intermittence is unusual.

The 'on' and 'off' probability distributions here refer to a single nanocrystal, time-averaged over ~ 1000 s with integration times typically over 100–150 ms [25]. In contrast, ensemble-averaged probability distributions depend strongly on nano-crystal packing and environment, varying between inverse power and stretched exponential decay [30,31]. The strongly non-ergodic behaviour of quantum dot intermittence implies a decisive role for dynamics. There are fluctuations in waiting times and sometimes even increases in waiting time averages at long times. This, with the power decay of the probability distributions, indicates Lévy, rather than Poisson or normal, statistics and puts constraints on the underlying physical processes [29]. Optical intermittence is often accompanied by spectral diffusion, that is, by variation in time of the shape and peak position of the absorption or fluorescence lines [25].

The accepted explanation of intermittent luminescence is that the dot changes charge state, with a neutral photoactive on-state and the dark off-states corresponding to a charged nanocrystal [23]. Early work suggested [23] that charging occurred via Auger processes: recombination following double excitation of a dot (producing $2e+2h$) could excite an electron into the surrounding matrix. This idea had support from two-photon adsorption studies. Later work failed to find the expected change in blinking kinetics at lower illumination intensity, prompting new models involving tunnelling of electrons from delocalized

dot states into localized traps in the environment [34] or at the dot–matrix interface [32,33]. These models can rationalise time dependences of the probability distributions for the off-states [34]. However, resonant tunnelling implies similar rates for tunnelling-out and tunnelling-in processes, leading to incorrect predictions for on-state statistics [35]. Tang and Marcus have suggested nanocrystal ionisation is diffusion limited [30,36,37]. We remark that, if one looks at the stochastic energy shifts, and assumes that these are associated with trapped electrons in the matrix, then these trapped electrons must be very close to the dot–matrix interface. These changes may damage the nanocrystal irreversibly [38]. Sometimes the behaviour is more complex, e.g. Hess et al [39] note a metastable dark state (possibly involving a surface transformation) is found on heating dots in solution or by changing the dot environment in certain other ways, with recovery possible with illumination. Further detailed studies demonstrated the blinking kinetics is altered by changing nanocrystals capping [32,40] or environment [25,41–43].

Whatever the mechanism of charging, it is clear that ionisation occurs much faster ($\sim \mu$s or faster) than fluorescence intermittency ($\sim$ seconds). Furthermore, the non-ergodic behaviour (inverse power decay of blinking distribution times) lasts even longer (10^2–10^3 s). There is still debate on the links between dynamical behaviour and the Levi long-time intermittence statistics. Novikov et al. [44] linked long-time memory phenomena with charge transport in ordered nanocrystal arrays, proposing transport is quasi-stationary and does not need a long-time dependence for individual dots. However, their model seems to disagree with recent data from Stefani et al. [45,46] suggesting substantial correlations between sequential on- and off-events of individual dots. Taken as a whole, the data on fluorescent intermittency suggest a complex interplay between short-time and long-time dot dynamics. It appears that fast but rare dynamical processes control long-time dynamics, and any adequate model must address this multiscale phenomenon.

3. Cycles of excitation and luminescence

In optical excitation and de-excitation cycles, there are several natural timescales. Optical excitation processes depend on the optical system and intensity, and largely under our control. There are then the natural timescales following excitation, and these determine operational timescales according to what it is we wish to do, e.g., to provide picosecond optical switch, exploiting the altered refractive index (polarisability) in the excited state.

Subsequent relaxation processes are of several distinct types. First, the redistribution of charge on excitation changes forces on the ions. In particular, the system must relax to eliminate surface shear stresses, since the vacuum cannot support shear. This [47] takes a time of the order of a picosecond, about the time for sound to cross the particle ([48] give an alternative way to estimate this timescale). One consequence is a dynamic dilation: volume change is roughly independent of dot size, so the fractional change (dilational strain) is inversely proportional to dot volume. This strain, and hence energy shifts associated with deformation potential coupling, are inversely proportional to dot volume, and can be significant. The elimination of shear stress does not need

energy redistribution, mainly changing the mean positions about which the system oscillates. There will be a *reduction* of dipole moment in the excited state [6] as the electron associates with the more positive regions and the hole with the more negative regions. Redistribution of energy is a second stage. "Cooling" processes (loss of energy from coherent motion in the configuration coordinate) competes with luminescence, non-radiative transitions and possible further electronic transitions, e.g., into so-called dark states.

3.1. Optical excitation cycle: cooling

We must distinguish two types of cooling following excitation. One type of cooling type establishes equilibrium among the different vibrational modes of the dot itself; the other takes energy from the dot as a whole, as the dot equilibrates with the surrounding matrix. One expects slower cooling for dots resting on a substrate than for those embedded in a matrix, simply because of diminished thermal contact. Even if a phonon temperature is established within a dot, it may differ from that of the surroundings, as in the spatial phonon bottleneck discussed by Eisenstein [49]. The amount of energy can be quite large: if a photon of 2 eV is absorbed by a dot of 100 atoms, and all subsequent transitions are non-radiative, then the added energy per atom corresponds to a temperature rise of 232°, and doubtless some modes are more strongly excited (higher effective temperature) than others. Even when light is emitted, there will be some cooling in the excited state before emission, and in the ground state after emission.

In a dot, the phonon system may equilibrate only slowly, i.e., a spectral bottleneck as energy is exchanged with what one might describe as the configuration coordinate, in analogy with colour centre studies. The configuration coordinate is not necessarily a normal mode, but rather a reaction coordinate (see [48] p 90). In the present case, it describes the vibrational relaxation towards equilibrium associated with coupling to the excitation. This gives a second class of cooling that is largely internal to the dot. Experimentally, one can discern hot luminescence [50,51]. The luminescence spectrum looks like a zero-phonon line of energy $\hbar\omega_0$ with sidebands. We might describe the dot vibronic behaviour with a configuration coordinate diagram in which the ground state has characteristic vibration frequency ω_g and excited state frequency ω_x. Emission can occur from excited electronic states with n_x phonons (we use the word "phonon" for clarity, even though it may not strictly correspond to a normal mode) to the ground electronic state with n_g phonons. This luminescent transition would have energy $\hbar\omega_0 + n_x \hbar\omega_x - n_g\hbar\omega_g$. Energies lower than $\hbar\omega_0$ correspond to transitions ending in a vibration-ally-excited ground state; energies higher than $\hbar\omega_0$ corre-spond to transitions from vibrationally-excited initial states, i.e., hot luminescence. The relative importance of hot lumines-cence gives some sort of measure of the transient temperature of the dot.

Analysis of data for small CdS dots [52] is in line with this description. The unrefined analysis of the sideband structure suggested a ground state phonon energy was around 32 meV, with the higher value of 35 meV in the excited state; both energies being fairly close to the 40 meV bulk LO phonon energy. The degree of thermal excitation at the time of luminescence was consistent with an energy input proportional to the laser intensity, and with cooling at an independent rate, so the dots did not cool instantly to the matrix temperature. A non-optimised analysis suggested temperature rises of order 100°. The zero phonon line will have contributions from all components with $n_x = n_g$, so there can be broadening and a shift as different components become important. In this case, this part of the shift would be to the blue, as $\hbar\omega_x > \hbar\omega_g$; however, there is also a red shift from thermal expansion. In the data analysed, thermal expansion dominated. The sideband intensities will also change in ways given by the Huang–Rhys model (see, e.g., [53,54] for the relevant formulae).

3.2. Electron–phonon coupling and Huang–Rhys factors

The data just described were consistent with Huang–Rhys factors of order 0.1–0.5, well in the ranges of published data [55]. Typically, the Stokes shift suggests a relaxation energy will be of order 0.1 eV, in line with a Huang–Rhys factor of 0.3 or so. Note that this analysis makes no assumptions about whether the excited states are simple effective mass states or charge transfer states. A number of calculations estimate the Huang–Rhys factor S as a function of dot radius. Most assume very simple initial and final wavefunctions, and most assume that the lattice vibrations and electron–phonon couplings are the same as for the bulk crystal (e.g., [56]). Few workers (an exception is Vasilevsky's treatment of dipolar vibration modes [57]) recognise the subtle but significant changes at the nanoscale, partly because of the boundary conditions. Usually, Fröhlich coupling to bulk-like longitudinal optic modes is presumed, and deformation potential and piezoelectric cou-plings to acoustic modes ignored. Simple analytical calculations are readily generalised ([58] following Ridley [59] and Stoneham [60]). The value of S depends on the form factors of the initial and final electronic states, with a particular distinction between states for which the boundary determines the wavefunction dimensions (e.g., when the dot radius is less than the exciton radius) and those for which a local interaction is dominant (e.g., a deep defect). S also depends on the wave-vector dependence of the electron–phonon coupling. In the most relevant cases (unscreened piezoelectric coupling, small dot radius R) the dependences are roughly $S \sim 1/R$ (Frohlich), $1/R^2$ (deformation potential) and R-independent (piezoelectric). De-pending on details, any one of these can dominate. Thus, when resonant Raman data suggest $S \sim 1/R$ (e.g., [61]) and photo-luminescence data indicate a similar result (CuCl dots in glass: [62] and CuBr [63]), this is open to several interpretations. The actual values of the Huang–Rhys factor will be sensitive to the properties of the interface between the dot and environment. First principles electronic structure calculations for the uncapped $(ZnS)_{47}$ cluster (Fig. 2) give rather large and similar ground and excited (triplet) state relaxation energies of 80 meV and 110 meV respectively, hence a Stokes shift of $\sim$ 190 meV. Given the bulk LO phonon energy of $\sim$ 48 meV, one obtains $S \sim 2$, i.e. inter-mediate coupling regime [64] rather than small coupling in the

discussed CdS analysis. However, a hole component of the exciton in this cluster of Fig. 2 is found to be strongly surface localized [6]. Chemical cupping and environment will certainly affect exciton relaxation and thus, Huang–Rhys factor.

4. Where the quantum enters: exploiting the excited state

The storage and manipulation of quantum information as qubits underpins successful quantum information processing. The underlying processes are frequently nanoscale and dynamic, as illustrated in the Stoneham–Fisher–Greenland proposal (SFG) [65]. This approach specifically exploits properties of impurities in silicon or silicon-compatible hosts. Electron spins are used as qubits, distributed *randomly* in space such that mutual interactions are small in the normal (ground) state, in which they are able to store quantum information. In an electronic excited state, however, entangling interactions between qubits can occur to manipulate pairs of qubits. Thus qubits are manipulated by magnetic fields and optical pulses. So how does this system invoke dynamics at the nanoscale?

First, quantum information processing will involve the dynamic and coherent manipulation of the spins: all the quantum manipulations must be done faster than decoherence processes. In the present case, decoherence comes primarily from spontaneous emission, photoionisation, spin lattice relaxation, and loss of quantum information to spins that should not be participating. Secondly, if we wish to entangle two spins, there is a characteristic range over which this is possible. In the SFG approach, the donors in their ground states are too far apart to interact (say 10 nm); an excited control electron can overlap two qubits through a shaped optical pulse to give a transient interaction. However, the wavelength of light (say 1000 nm, or 1 μm) is so long that it is not possible to focus on just one chosen pair of qubits. To address individual gates, one exploits spatial and spectroscopic selectivity. The natural disorder and spatial randomness in doped semiconductors is crucial. Basically, the laser system can focus on (say) one square micron. Within this, simply because the spacings of the donors and control dopants are random, the excitations to manipulate qubits will have different energies from one qubit pair to another. Randomness is beneficial.

As described, there is a limit to the number of qubits in one square micron that can be linked from the spectral bandwidth available. With sensible values, this would be about 20 qubits. One would like to be able to link say 250 qubits. Can this be done? We can imagine "patches" of say 20 gates in a small zone (perhaps 100 nm across) of each micron-sized region. We need a means to transfer quantum information from one patch to another, a "flying qubit". We have specific ideas as to how to achieve this in a way compatible with silicon technology and with our wish to operate devices at room temperature, but will not be discussed here. A linked set of say 12 patches, each containing 20 qubits, would give 240 qubits. However, we remark that links between patches may be less efficient than qubit manipulations within a patch, so there are implications for efficient algorithms.

If there is to be widespread use by the public, the processor should operate at room temperature, alongside conventional classical devices. It should link well with conventional silicon-based

microelectronics. Classical microelectronics dominates current information processing, and continues to evolve in a truly impressive way; it will not be replaced by quantum information processing; rather, quantum behaviour will extend its range of possibilities. Any quantum information processors are likely to be controlled by classical microelectronic devices. There are therefore strong reasons to look for quantum information processors that are themselves silicon-based. As the optically-controlled SFG quantum gates do not rely on small energy scales, they might function at or near room temperature. Likewise, decoherence mechanisms should permit operation at useful temperatures. Quantum behaviour is not intrinsically a low-temperature phenomenon. Quantum behaviour is evident in two main ways. In quantum statistics, the quantal $\hbar$ appears in combinations like $\hbar\omega/kT$, and it is certainly true that high temperatures make quantal effects less and less evident. But statistics relate primarily to equilibrium behaviour. In quantum dynamics, $\hbar$ appears without T, and indeed the quantum role may be to open new channels. Quantum information processing relies on dynamics and staying far from equilibrium. There is no *intrinsic* problem with high temperatures. Practical issues may be another matter, of course, since the rate of approach to equilibrium tends to be faster at higher temperatures.

5. Scent molecule: nasal receptor

Nanoscience covers both physical and biological systems. In many life processes, molecules interact with receptors. These receptors are highly specific and selective, and their actuation initiates important biophysical phenomena. The molecules might be small molecules, neurotransmitters, like NO or serotonin, or large molecules, like many enzymes. For large molecules, shape (in the general sense, including distribution of adhesive patches) is a major factor. Indeed, it is almost a mantra
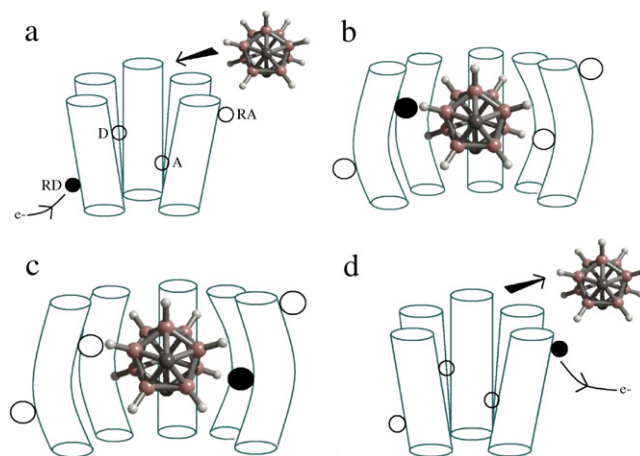

Fig. 4. Schematic illustration of the Turin mechanism. (a) The olfactory receptor, a barrel structure formed from polypeptide chains. Inelastic tunnelling will occur between donor D and acceptor A. The two "reservoirs" RD and RA ensure that there is an electron on D and that the electron is removed after tunnelling to A. (b) The scent molecule enters the receptor, deforming it. (c) Inelastic electron tunnelling occurs, with the excitation of a vibration of the scent molecule. (d) The scent molecule leaves and the system re-initialises.

that there is a "lock and key" mechanism in which shape is the only factor, despite lack of clarity about actuation (the key needs to be turned in a human-scale lock). For small molecules, whilst shape may be necessary, it is certainly not sufficient. More is needed to understand what actuates the receptor, immediately after the molecule arrives. One suggestion [66] is a "Swipe Card" model: your human-scale Swipe Card has to fit well enough, but it is something other than shape (often magnetic for swipe cards) that transfers information and actuates the system. At the molecular scale, it might be *proton transfer* (perhaps for serotonin, [67]), or *inelastic electron tunnelling* for scent molecules as suggested by Turin [68]). We outline some of the processes in Turin's model of olfaction, following [69]. In the swipe card model, there is a natural actuation event, e.g., electron or proton transfer.

Scent molecules are small, rarely more than 50 atoms in size, and will each interact with a number of different receptors, from whose signals the brain discerns a particular scent. Evidence that shape is inadequate to explain observation includes the existence of olfactants that are structurally similar but smell different (e.g, ferrocene smells spicy, and nickelocene has an oily chemical smell) and olfactants that smell the same but are structurally dissimilar. Turin noted that those olfactants that smell the same, even if chemically very different (e.g., decaborane and hydrogen sulphide) have similar vibrational frequencies. He made the imaginative proposal that the nasal receptor might discern different vibrational frequencies by inelastic tunnelling. Thus a receptor would have a donor component and an acceptor component (Fig. 4a). Without the olfactant, no tunnelling occurs, either because the tunnelling distance is too large or the energies do not match. When the olfactant is present, tunnelling conserves energy by emission of an odorant vibration of definite energy; there is no elastic channel that conserves energy. This is an oversimplified outline of a sequence of processes Fig. 4 that have been analysed in a quantitative model by Brookes et al [69].

Full scale electronic structure calculations on the small olfactant molecule are practical. Any model has to accept that receptor structures are not known with any certainty, and certainly not to better than ~2 Å, whereas tunnelling may be sensitive to changes of 0.1 Å. However, there are well-defined constraints and there is information on other parameters from other biomolecules. No special electronic resonances of receptor and molecule are needed. It is possible to verify that the Turin model could work with sensible values of all parameters, i.e., there is nothing *un*physical in the model. The detailed analysis suggests interesting features of the receptor that warrant further attention and experiments.

There are then the various challenges to the Turin theory. Shouldn't enantiomers (chiral odorants with left- and right-handed forms) smell the same, since their vibrations are the same (whereas shape theories would say all should smell different)? Experimentally, the extensive Leffingwell lists [70] suggest about half such pairs smell the same, and about half smell different. Within the Turin picture, those that smell different do so because there are different intensities from left- and right-handed forms, and these different intensities are determined in

part by shape factors. Shouldn't there be an isotope effect, as changing H for D would alter frequencies? This is still controversial. Some authors say there is no difference; others say that humans, dogs and rats can discern isotope differences. There are experimental difficulties as well, since there can be isotope exchange and other isotope-related reactions in the nose, and the definitive experiment has not been done.

It is interesting that many of the processes (electron transport; electron tunnelling; deformation of the receptor by the olfactant; thermal fluctuations) are relatively slow; after all, scent is discerned on a timescale no faster than ms. But all involve dynamics at the nanoscale. Indeed, the swipe card description – which is a new paradigm for receptor processes, with possibly very wide application – is naturally dynamic and nanoscale.

6. Conclusions

Behaviour at the nanoscale presents some generic challenges [71]. A first challenge is to identify just what are the most important scientific ingredients. The temptation is to assume the significant questions are the familiar questions. The second challenge is how to bring together a mix of computer-based, analytical, and statistical theories to address these key issues. The temptation for those used to macroscopic theory is to believe nanoscience is miniaturised macroscience; for those used to the atomic scale, the temptation is to believe that it suffices to extend familiar atomistic ideas. The third challenge is how to understand the link between structure and performance. The temptation is to believe that structures which look alike will actually behave alike, when even one extra atom can make a difference. But perhaps the fourth challenge is the most important: process is more significant than structure. Structures are not validated by appearance alone, but by how they perform. Knowledge of ground-state energies for idealised systems, crystal structures and surface reconstructions is only a beginning.

Dynamics is an unavoidable ingredient at the nanoscale, whether the movement is electronic, a near-equilibrium fluctuation, or a subtle biological process. Depending on the system, the creation of nanostructures can range from slow, near equilibrium processes to rapid and complex picosecond dynamics, far from equilibrium, and substantially decoupled from the environment. The observed dynamics will reflect the fact that even nominally identical nanostructures are rarely identical, since self-organisation is usually imprecise, and apparently minor differences can have significant consequences. Behaviour can be non-ergodic, for instance, with ensemble and time averages different. The efficiency of equilibration of a nanostructure with its host can vary greatly with details. Sometimes rapid equilibration is desirable, for instance in removing heat from a catalyst particle for an exothermic reaction. At other times, slow equilibration is desirable, as when one wishes to preserve the phase of an electron, phonon or quantum state. Any one system may have important dynamics on both short and long timescales, and the interplay between the two is to be found in many systems.

Our examples have aimed to illustrate the range of dynamic phenomena and, in particular, to identify cases where there are

surprises. If we were to identify themes that we regard as especially important in the next stages of nanoscale science, then we would note four personal choices. The first theme involves the ways in which living organisms exploit hard and soft matter with such ingenuity. Our example of olfaction attempts to understand such remarkable biological phenomenon. A second theme might be the exploitation of selective electronic excitation: the use of spatial and spectral resolution together for low thermal budget nanoprocessing, as well as for quantum information processing. A third theme is the significance of coherence, whether vibrational, electronic or quantum. The final theme, and the main thrust of this paper, is the need to recognise that, at the nanoscale, dynamics dominates the system's behaviour.

Acknowledgements

References

[1] A.M. Stoneham, J.H. Harding, Nat. Mater. 2 (2003) 77.
[2] P. Williams, E. Keshavarz-Moore, P. Dunnill, Enzyme Microb. Technol. 19 (1996) 208.
[3] M.T. Klem, M. Young, T. Douglas, Mater. Today (Sept 2005) 28.
[4] D. Ishli, K. Kinbara, Y. Ishida, N. Ishil, M. Okochi, M. Yohda, T. Alda, Nature 423 (2003) 629.
[5] A.M. Stoneham, Solid State Commun. 3 (1965) 71.
[6] J.L. Gavartin, A.M. Stoneham, Philos. Trans. R. Soc. Lond., A 361 (2003) 275.
[7] J. Fritcsh, P. Pavone, Surf. Sci. 344 (1995) 159.
[8] A.I. Screbtii, R. Di Felice, C.M. Bertoni, R. Del Sole, Phys. Rev., B 51 (1995) 11201.
[9] G. Kresse, J. Furthmüller, Comput. Mater. Sci. 6 (1996) 15.
[10] G. Kresse, J. Hafner, Phys. Rev., B 49 (1994) 14251.
[11] G. Kresse, J. Furthmüller, Phys. Rev., B 54 (1996) 11169.
[12] T.K. Tran, W. Park, W. Tong, M.M. Kyi, B.K. Wagner, C.J. Summers, J. Appl. Phys. 81 (1997) 2803.
[13] P. Buffat, Philos. Trans. R. Soc. Lond. Ser. A: Math. Phys. Sci. 361 (2003) 291.
[14] W.A. Philips, Rep. Prog. Phys. 50 (1987) 1657.
[15] K. Trachenko, M.T. Dove, K.D. Hammonds, M.J. Harris, V. Heine, Phys. Rev. Lett 81 (1998) 3431.
[16] A.M. Stoneham, A.H. Harker, in press.
[17] V.V. Yakovlev, V. Lazarov, J. Reynolds, M. Gajdardziska-Josifovska, Appl. Phys. Lett. 76 (2000) 2050.
[18] K. Sattler, J. Mühlbach, O. Echt, P. Pfau, E. Recknagel, Phys. Rev. Lett. 47 (1981) 160.
[19] A. Franceschetti, A. Zunger, Phys. Rev., B 62 (2000) R16287.
[20] D. Regelman, E. Dekel, D. Gershoni, E. Ehrenfroind, A.J. Williamson, J. Shumway, A. Zunger, Phys. Rev., B 64 (2001) 165301.
[21] V.I. Klimov, Ch.J. Schwarz, D.W. McBranch, C.A. Leatherdale, M.G. Bawendi, Phys. Rev., B 60 (1999) R2177.
[22] M. Nirmal, D.J. Norris, M. Kuno, M.G. Bawendi, Al.L. Efros, M. Rosen, Phys. Rev. Lett. 75 (1995) 3728.
[23] M. Nirmal, B.O. Daboussi, M.G. Bawendi, J.J. Mackin, J.K. Trautman, T.D. Harris, L.E. Brus, Nature 383 (1996) 802.
[24] C. Delerue, M. Lannoo, G. Allan, E. Martin, I. Mihalcescu, J.C. Vial, R. Romestain, F. Muller, A. Bsiesy, Phys. Rev. Lett. 75 (1995) 2228.
[25] K.T. Shimizu, W.K. Woo, B.R. Fisher, H.J. Eisler, M.G. Bawendi, Phys. Rev. Lett. 89 (2002) 117401.
[26] J.J. Peterson, T.D. Krauss, Nano Lett. 6 (2006) 510.
[27] F. Chichos, J. Martin, C. von Borczyskowski, Phys. Rev., B 70 (2004) 115314.
[28] K. Matsuda, Y. Kanemitsu, K. Irie, T. Saiki, T. Someya, Y. Miyauchi, S. Maruyama, Appl. Phys. Lett. 86 (2005) 123116.
[29] E. Barkai, Y. Jung, R. Silbey, Annu. Rev. Phys. Chem. 55 (2004) 457.
[30] I. Chung, M.G. Bawendi, Phys. Rev., B 70 (2004) 165304.
[31] J. Tang, R.A. Marcus, J. Chem. Phys. 123 (2005) 204511.
[32] N.I. Hammer, K.T. Early, K. Sill, M.Y. Odoi, T. Emrick, M.D. Barnes, J. Phys. Chem., B 110 (2006) 14167.
[33] P.A. Frantsuzov, R.A. Marcus, Phys. Rev., B 72 (2005) 155321.
[34] K.T. Shimizu, R.G. Neuhauser, C.A. Leatherdale, S.A. Empedocles, W.K. Woo, M.G. Bawendi, Phys. Rev., B 63 (2001) 205316.
[35] D.P. Fromm, S.T. Johnson, A. Gallagher, D.J. Nesbitt, Phys. Rev., B 67 (2003) 125304.
[36] J. Tang, R.A. Marcus, Phys. Rev. Lett. 95 (2005) 107401.
[37] J. Tang, R.A. Marcus, J. Chem. Phys. 125 (2006) 044703.
[38] S.A. Blanton, M.A. Hines, P. Guyot-Sionnest, Appl. Phys. Lett. 69 (1996) 3905.
[39] B.C. Hess, I.G. Okhrimenko, R.C. Davis, B.C. Stevens, Q.A. Schlulzke, K.C. Wright, C.D. Bass, C.D. Evans, S.L. Summers, Phys. Rev. Lett. 86 (2001) 3132.
[40] J. Muller, J.M. Lupton, A.L. Rogach, J. Feldmann, D.V. Talapin, H. Weller, Phys. Rev., B 72 (2005) 205339.
[41] R. Verberk, J.W.M. Chon, M. Gu, M. Orrit, Physica, E, Low-Dimens. Syst. Nanostruct. 26 (2005) 19.
[42] Z. Gueroui, A. Libchaber, Phys. Rev. Lett. 93 (2004) 166108.
[43] J. Schuster, F. Cichos, C. Von Borczyskowski, Opt. Spectrosc. 98 (2005) 712.
[44] D.S. Novikov, M. Drndic, L.S. Levitov, M.A. Kastner, M.V. Jarosz, M.G. Bewendi, Phys. Rev., B 72 (2005) 075309.
[45] F.D. Stefani, X.H. Zhong, W. Knoll, M.Y. Han, M. Kreiter, New J. Phys. 7 (2005) 197.
[46] F.D. Stefani, W. Knoll, M. Kreiter, X.H. Zhong, M.Y. Han, Phys. Rev., B 72 (2005) 125304.
[47] A.M. Stoneham, B. McKinnon, J. Phys., Condens. Matter 10 (1998) 7665.
[48] N. Itoh, A.M. Stoneham, Materials Modification by Electronic Excitation, Cambridge University Press, 2001.
[49] J. Eisenstein, Phys. Rev. 84 (1951) 548.
[50] J. Tittel, W. Gohde, F. Koberling, T. Basche, A. Kornowski, H. Weller, A. Eychmuller, J. Phys. Chem., B 101 (1997) 3013.
[51] A. Mews, Private Communication 1999.
[52] A.M. Stoneham. 1999, unpublished analysis.
[53] K. Huang, A. Rhys, Proc. R. Soc. Lond., A 204 (1950) 406.
[54] A.M. Stoneham, Theory of Defects in Solids, Oxford University Press, 1975.
[55] U. Woggon, Optical Properties of Semiconductor Quantum Dots, Springer, Berlin, 1997.
[56] A.V. Fedorov, A.V. Baranov, Sov. Phys. JETP 83 (1996) 610.
[57] M.I. Vasilevsky, Phys. Rev., B 66 (19) (2002) 5326.
[58] B.K. Ridley, A.M. Stoneham, J.L. Gavartin, in press.
[59] B.K. Ridley, Quantum Processes in Semiconductors, Oxford University Press, 2000.
[60] A.M. Stoneham, J. Phys. C 12 (1979) 891.
[61] A.V. Baranov, S. Yamauchi, Y. Masumoto, Phys. Rev., B 56 (1997) 10332.
[62] T. Itoh, M. Nishijima, A.I. Ekimov, C. Gourdon, A.L. Efros, M. Rosen, Phys. Rev. Lett. 74 (1995) 1645.
[63] K. Inoue, A. Yamanaka, K. Toba, A.V. Baranov, A.A. Onushchenko, A.V. Fedorov, Phys. Rev., B 54 (1996) 8321.
[64] A.D. Yoffe, Adv. Phys. 50 (2001) 1.

[65] A.M. Stoneham, A.J. Fisher, P.T. Greenland, J. Phys., Condens. Matter 15 (2003) L447.
[66] A.M. Stoneham, in press.
[67] D. Wallace, A.M. Stoneham, A. Testa, A.H. Harker, M.M.D. Ramos, Mol. Simul. 2 (1993) 385.
[68] L. Turin, Senses 21 (1996) 773.
[69] J. Brookes, F. Hartoutsiou, A. Horsfield, A.M. Stoneham, 2006 in preparation.
[70] J.C. Leffingwell, Leffingwell Rep. 5 (2001) 1.
[71] A.M. Stoneham, Mater. Sci. Eng., C, Biomim. Mater., Sens. Syst. 23 (2003) 235.